Exp.-Nr. **A2-04/09**
Eingang: 15.05.2009
an PAC: 18.05.2009

Mainz Microtron MAMI

Collaboration A2: "Tagged Photons"
Spokesperson: A. Thomas

Proposal for an Experiment

"Induced neutron polarisation from the photo-disintegration of the deuteron"

Spokespersons for the Experiment :
J.R.M. Annand (Department of Physics and Astronomy, University of Glasgow)
P. Grabmayr, D.G. Middleton (Physikalisches Institut, Universität Tübingen, Tübingen)

Abstract of Physics :

We propose to measure the induced neutron polarisation from the photo-disintegration of the deuteron at over a wide range of incident photon energies. Such a measurement will provide further information regarding the NN-interaction and serve as further tests of existing theoretical models. These models, based on meson-baryon degrees of freedom, are currently unable to describe a large peak that has previously been observed in the induced proton asymmetry at for incident photon energies of roughly 400 - 800 MeV. Ascertaining whether such a peak exists in the asymmetry would be of great value in trying to understand the nature of the observed peak and provide more information for the development of future models.

Abstract of Equipment :

The experiment will be performed at the tagged photon facility of MAMI (Glasgow-Tagger). A second experimental area downstream of the crystal ball will be used with wire chambers and a scintillator detector for detection of the proton plus two other sets of scintillator detectors for analyser and polariser of the recoiling neutron.

MAMI Specifications :

beam energy	855 MeV
beam current	< 20 nA
beam polarisation	polarised

Photon Beam Specifications :

tagged energy range	200 - 500, 400 - 800 & 500 - 800 MeV
photon beam polarisation	circularly polarized

Equipment Specifications :

detectors	TOF, Basel scintillator detector, analyser scintillator detctor, wire chambers.
target	10 cm liquid deuterium

Beam Time Request :

set–up/tests with beam	150 hours (parallel with proposal A2/03-09)
data taking	400 hours (parallel with proposal A2/03-09)

List of participating authors:

- **Institut für Physik, University of Basel, Switzerland**
  I. Jaegle, I. Keshelashvili, B. Krusche, Y. Maghrbi, F. Pheron, T. Rostomyan, D. Werthmüller
- **Institut für Experimentalphysik, University of Bochum, Germany**
  W. Meyer, G. Reicherz
- **Helmholtz–Institut für Strahlen- und Kernphysik, University of Bonn, Germany**
  R. Beck, A. Nikolaev
- **Massachusetts Institute of Technology , Cambridge, USA**
  A. Bernstein, W. Deconinck
- **JINR, Dubna, Russia**
  N. Borisov, A. Lazarev, A. Neganov, Yu.A. Usov
- **School of Physics, University of Edinburgh, UK**
  D. Branford, D.I. Glazier, T. Jude, M. Sikora, D.P. Watts
- **Petersburg Nuclear Physics Institute, Gatchina, Russia**
  V. Bekrenev, S. Kruglov, A. Koulbardis
- **Department of Physics and Astronomy, University of Glasgow, UK**
  J.R.M. Annand, D. Hamilton, D. Howdle, K. Livingston, J. Mancell, J.C. McGeorge, I.J.D. MacGregor, E.F. McNicoll, R.O. Owens, J. Robinson, G. Rosner
- **Department of Astronomy and Physics, Saint Mary's University Halifax, Canada**
  A.J. Sarty
- **Kent State University, Kent, USA**
  D.M. Manley
- **University of California, Los Angeles, USA**
  B.M.K. Nefkens, S. Prakhov, A. Starostin, I.M. Suarez
- **MAX-lab, University of Lund, Sweden**
  L. Isaksson
- **Institut für Kernphysik, University of Mainz, Germany**
  P. Aguar-Bartolome, H.J. Arends, S. Bender, A. Denig, E.J. Downie, N. Frömmgen, E. Heid, O. Jahn, H. Ortega, M. Ostrick, B.Oussena, P.B. Otte, S. Schumann, A. Thomas, M. Unverzagt
- **Institut für Physik, University of Mainz, D**
  J.Krimmer, W.Heil
- **University of Massachusetts, Amherst, USA**
  P.Martel, R.Miskimen
- **Institute for Nuclear Research, Moscow, Russia**
  G. Gurevic, R. Kondratiev, V. Lisin, A. Polonski
- **Lebedev Physical Institute, Moscow, Russia**
  S.N. Cherepnya, L.V. Fil kov, V.L. Kashevarov
- **INFN Sezione di Pavia, Pavia, Italy**
  A. Braghieri, A. Mushkarenkov, P. Pedroni
- **Department of Physics, University of Regina, Canada**
  G.M. Huber

- **Mount Allison University, Sackville, Canada**
  D. Hornidge
- **Tomsk Polytechnic University, Tomsk, Russia**
  A. Fix
- **Physikalisches Institut, University of Tübingen, Germany**
  P. Grabmayr, T. Hehl, D.G. Middleton
- **George Washington University, Washington, USA**
  W. Briscoe, T. Morrison, B.Oussena, B. Taddesse, M. Taragin
- **Catholic University, Washington, USA**
  D. Sober
- **Rudjer Boskovic Institute, Zagreb, Croatia**
  M. Korolija, D. Mekterovic, S. Micanovic, I. Supek

1 Introduction

At present QCD in the non-perturbative regime can currently only be described using effective degrees of freedom. Frameworks of nucleons, mesons and isobars, whose properties are either described phenomenologically or by effective quark models, are used. The accuracy of this effective description and where it can be applied before quark-gluon degrees of freedom have to be considered is a question which is of great interest in modern nuclear physics. The main points of interest therefore are the role of meson and isobar degrees of freedom in medium energy reactions, many-body phenomena induced by the effective description in terms of hadronic degrees of freedom and the properties of the neutron or the use of light nuclei as an effective neutron target.

The use of electromagnetic reactions on few nucleon systems can help to shed light on these questions. For the lightest stable nuclei, ^{2}H, ^{3}He, reliable theoretical descriptions are available which do not depend on approximations that are necessary for more complex many-body systems [1, 2, 3]. These nuclei therefore make good test laboratories for the investigation of these effective degrees of freedom and their interaction. Also reactions above pion threshold are of particular interest to study meson degrees of freedom and internal baryon structure with the use of these nuclei as effective neutron targets. Furthermore the electromagnetic interaction is well known and sufficiently weak to allow conclusive interpretations in terms of charge and current matrix elements to be drawn.

The NN-interaction is an important ingredient for calculations for heavier nuclei. Comparison of recent measurements of the ^{3}He*(e,e′pp)* and ^{3}He*(e,e′pn)* reactions to theoretical calculations of the cross section which use the Faddeev technique [4] showed large discrepancies between results for the two reactions [5, 6]. Figure 1 shows the missing momentum cross sections for both the ^{3}He*(e,e′pp)* and ^{3}He*(e,e′pn)* reactions for a similar kinematic setting compared to theoretical calculations of the cross sections. As can be seen for the *(e,e′pp)* measurement the theoretical predictions under-predict the measured data but there is reasonable agreement between the two cross sections in the low missing momentum region though not at high missing momentum. For the *(e,e′pn)* measurement the theoretical cross sections over-predict the measured ones by a factor 5 at low missing momentum but show reasonable agreement within the large statistical error bars at high p_m. This discrepancy between the two comparisons is interpreted as being partly due to the influence of exchange currents on the reaction and final state interactions (FSI), the effect of which is believed to be substantial on both cross sections of both reactions in view of the results seen in [7]. Due to the problems associated with the interpretation of data from measurements using ^{3}He (and heavier target nuclei) one should therefore use the deuteron to improve understanding of the NN-interaction before trying to study it in more complex nuclei.

Photo- and electro-disintegration of the deuteron has been studied for many years both experimentally and theoretically and is still much studied today. Many aspects of the reaction, including studies of different polarisation observables, covering a wide range of incident (virtual) photon energies have been carried out to better understand the underlying reaction processes involved and reviews of the available experimental data and theoretical models can be found in [8, 9]. Generally there is now good agreement between the experimental measurements and the theoretical calculations developed to describe these experimental data for the energy ranges where the models are applicable.

At medium incident photon energies (from π-threshold to about 500 MeV) H. Arenhövel and M. Schwamb have developed a detailed theory [1, 10, 11] of deuteron photodisintegration. The calculations use a coupled-channel approach which includes the NN,

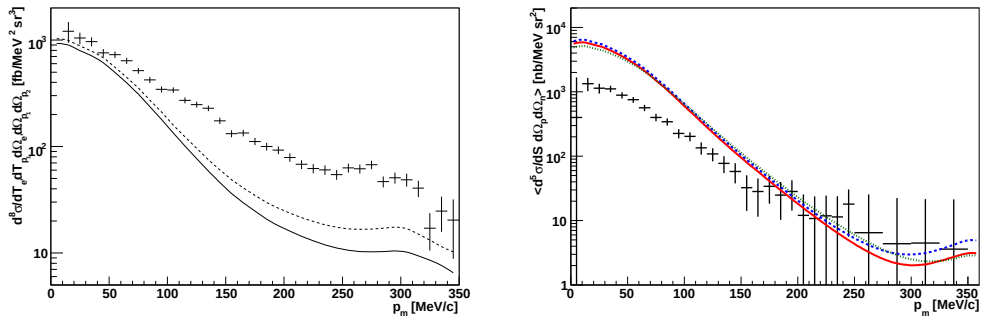

Figure 1: Cross sections from the ^{3}He$(e,e'pp)$ (left) and ^{3}He$(e,e'pn)$ (right) reactions shown as a function of the missing momentum of the reaction. In the $(e,e'pp)$ plot the solid curve is a theoretical calculation of the cross section using only a one-body current hadronic current operator with the Bonn-B NN-potential; the dashed curve further includes MECs in the calculations. In the $(e,e'pn)$ plot the solid curve is a theoretical calculation of the cross section using only a one-body current hadronic current operator with the Argonne $V18$ NN-potential; the dashed curve further includes meson exchange currents in the calculations. The dotted curve uses only a one-body current hadronic current operator with the Bonn-B NN-potential.

$N\Delta$, and πD channels as well as contributions from meson retardation and meson exchange currents. All of the parameters used in the model are fixed from nucleon-nucleon scattering and photo-reaction data and are not varied to fit deuteron photo-disintegration observables. The calculations show generally good agreement with experimental data for the applicable energy range although significant discrepancies with some polarisation observables remain.

There also exist unpublished calculations of the Bonn group [12, 13] for deuteron photo-disintegration which extend to higher incident photon energies, ∼1.5 GeV. The calculations include pole diagrams generated from π, ρ, η, and ω exchange plus seventeen well-established N^* and Δ resonances with mass less than 2 GeV and $J \leq 5/2$. The calculations use resonance parameters taken from the Particle Data Group [9]. These calculations do not in general show as good agreement with the measured data as those of Schwamb and Arenhövel, particularly at lower photon energies. Qualitatively the calculations show the same shape as experimental data for some observables but tend to wrongly predict the measured strength.

The Moscow-Tübingen theory group has developed a nucleon-nucleon potential which apart from the NN-part also contains a Fock column describing a $6q + meson$ component, where the $6q + \sigma$ play a significant part [14, 15, 16]. This so-called dibaryon model gives consistent explanation of the character of short-range NN correlations in the deuteron [17, 18] and of NN scattering observables at energies up to 1 GeV [19, 20]. The model explains quantitatively, without any free parameters, the magnetic form factor of deuteron, $B(q^2)$, in the area of the diffraction minimum [17] and also the circular polarisation of photons produced in the inverse $\vec{n}p \to d\gamma$ process [18]. Presently, the group is developing a wave packet description of reactions [21] of which deuteron photo-disintegration will be one of the first applications.

Figure 2 shows data from a measurement of the total cross section for deuteron photo-disintegration compared to calculations of Arenhövel and Schwamb [1]. The solid curve should be compared with the data. The different curves use different static and retarded coupled channel approaches for descriptions of meson exchange and more details of these

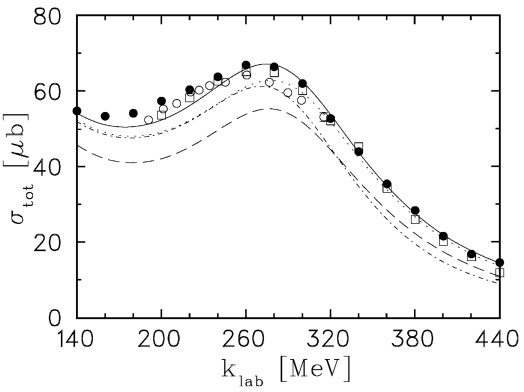

Figure 2: The total cross section for deuteron photo-disintegration as a function of the incident photon energy, taken from [1]. The data are taken from [22] (filled squares), [23] (empty squares) and [24, 25] (empty circles) and should be compared to the solid curve. See [1] for more details on the different theoretical curves.

can be found in [1]. As can be seen in figure 2 the experimental data is of good quality and is very well described by the calculations except at photon energies just above π-threshold where there is a slight under-prediction of the measured data points. Further good agreement is seen in figure 3 which shows data from measurements of the differential cross section of deuteron photo-disintegration as a function of of the c.m. proton angle, θ_p, for a range of incident photon energy bins. The notation of the data points and theoretical curves are the same as in figure 2. Again the experimental data are generally well described by the calculations for all beam energies though at higher photon energies the quality of the data is not good. Similarly to the comparison to the total cross section data there is a slight under-prediction of the data at the lower photon energies centred around $\theta_p = 90°$.

There have also been many measurements of the photon asymmetry, Σ. Figure 4 shows the results of some of these measurements as a function of of the c.m. proton angle, θ_p, for a range of incident photon energy bins. For photon energies where the data is of good quality there is reasonable agreement between the measured data points and the theoretical curves. At lower photon energies there is a slight under-prediction of the measured asymmetries around $\theta_p = 90°$, similar to what was seen for the differential cross sections in figure 3.

The induced polarisation of the proton is another observable that has exhibited some intriguing behaviour when compared to theoretical models. Initial measurements at SLAC [28] and Bonn [29] were followed up by measurements at Tokyo [30, 31] and many measurements at Kharkov [32, 33, 34, 35, 36, 37, 38, 39, 40] and more recently by measurements at JLab [41, 42] which greatly extended the incident photon energy range covered. Many of these data points can be seen in figure 5 which shows P_y^p for a range of incident photon energies for c.m. proton angle $\theta_p = 90°$ compared to two calculations of the asymmetry, see the figure caption for details of the data points and theoretical curves.

In figure 5 the experimental data show an increase in the asymmetry from about 200 MeV to about 500 MeV before it starts to decrease with increasing photon energy. There is some discrepancy between the different measurements regarding the magnitude of the asymmetry at the peak and also at energies above ~600 MeV where the Kharkov data show a dip in the asymmetry before it once more increases while the Tokyo and JLab data show the asymmetry tending to zero at higher photon energies. The authors of the review from which this figure was taken [9] conclude that due to the experimental set-up used in the Kharkov measurements the highest energy data set is unreliable and that the

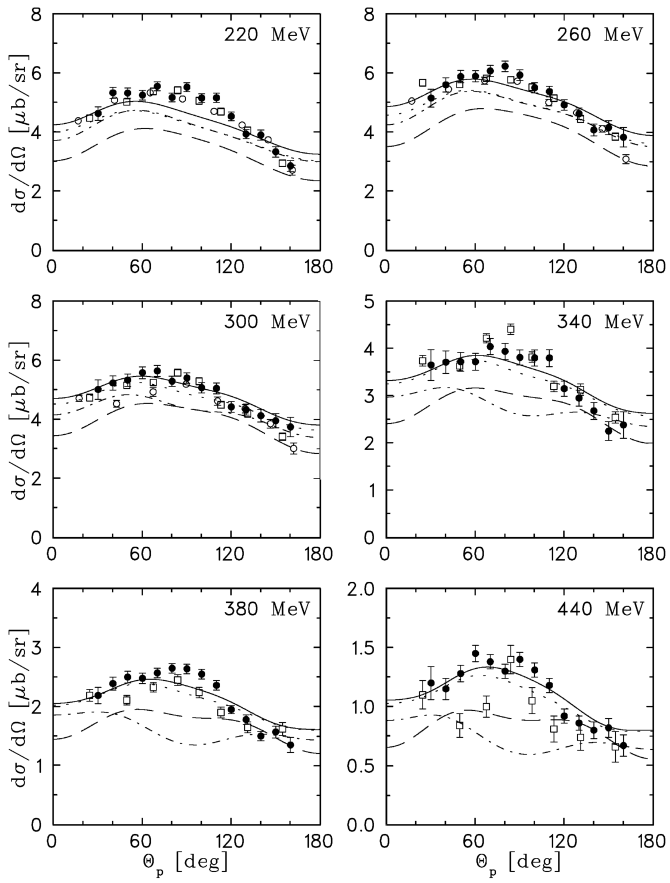

Figure 3: Differential cross sections of deuteron photo-disintegration as a function of the c.m. proton angle, θ_p, for a range of incident photon energies taken from [1]. Notation is the same as in fig. 2. The solid curve represents the full calculation.

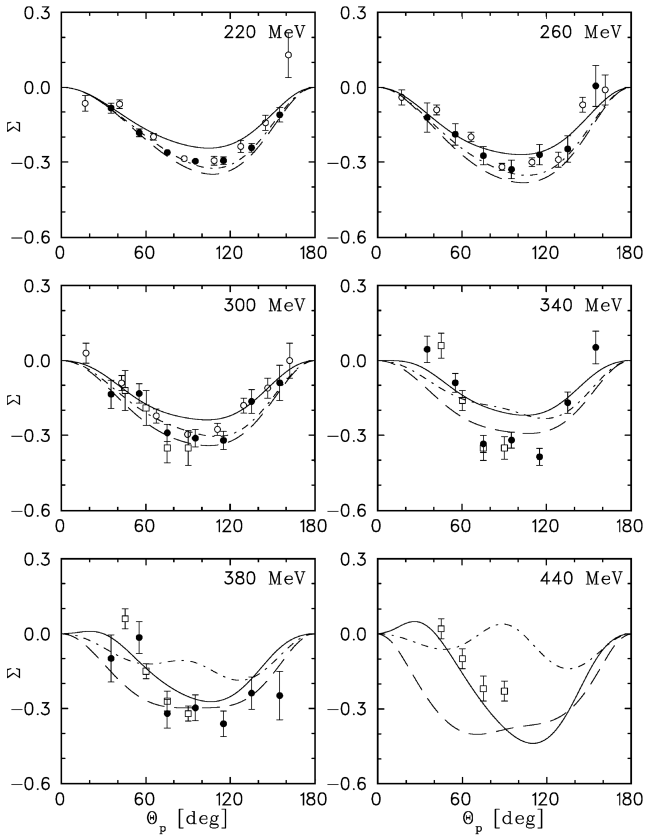

Figure 4: The Σ asymmetry for photo-disintegration of the deuteron shown as a function of the c.m. proton angle, θ_p, for a range of incident photon energies taken from [1]. The data are from [24, 25] (empty circles), [26] (filled circles) and [27] (empty squares). The theoretical curves are taken from [1] though the notation is different to figures 2 and 3, please see [1] for more details. The data should be compared to the solid curve.

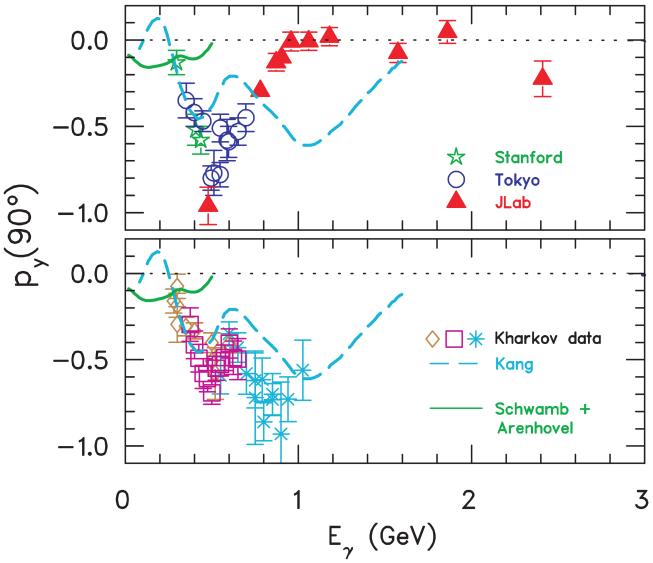

Figure 5: The induced neutron polarisation P_y^p for photo-disintegration of the deuteron shown as a function of the incident photon energy for c.m. proton angle $\theta_p = 90°$ taken from [9]. The data are from [28] (stars), [31] (circles) and [41] (triangles) in the top panel and [34] (diamonds), [37] (squares) and [36] (stars) in the bottom panel. Theoretical curves are from Schwamb [1] (solid) and Kang [12] (dashed).

JLab data should be believed for photon energies above ∼600 MeV.

The theoretical curve from the calculations of Schwamb and Arenhövel do not show good agreement with the measured data for this observable for the region they are applicable. Their calculations show a decrease in the asymmetry for photon energies above ∼200 MeV while all the data shows a clear increase. The calculations of Kang *et al.* [12, 13] show reasonable agreement up to about 400 MeV but fail to reproduce the large asymmetry at 500 MeV and also the shape of the JLab data at higher energies. Although these calculations do reproduce the qualitative features of the Kharkov data as stated above it is believed that these data are unreliable when compared with the more recent JLab data.

This peak in induced asymmetry at about 500 MeV incident photon energy is quite interesting in that it is not reproduced by either of the calculations available. In the eighties when many of the measurements shown in figure 5 were carried out there was much interest in the possibility of the existence of dibaryon resonances and it was believed that this peak in P_y^p was evidence for this. In [43] a partial wave analysis of the data was made which predicted the existence of at least two dibaryon resonances which could be excited in the photon energy region 350 - 700 MeV. Whether such states exist or not the inability of models to describe P_y^p is intriguing and warrants more investigation.

M. Schwamb believes the failure of his model to correctly predict the P_y^p asymmetry could be due to the fact that some partial waves which usually have a small effect in the NN-FSI which are not described well in his approach might be very important for this variable [44]. If so the model will also fail to reproduce the P_y^n asymmetry if there is a similar large peak observed. Therefore it would also be interesting to see whether such behaviour is also observed in the P_y^n asymmetry. Investigation into the presence of this peak in some of the possible double polarisation channels would also be highly desirable as further tests of existing models.

There have been no explicit measurements of P_y^n carried out for the energy range of

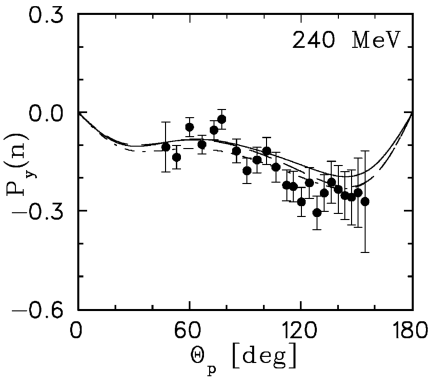

Figure 6: The induced neutron polarisation P_y^n for photo-disintegration of the deuteron shown as a function of the c.m. proton angle, θ_p, for a range of incident photon energies. The data are from [45] and the theoretical curves from [1]. The data should be compared to the solid curve.

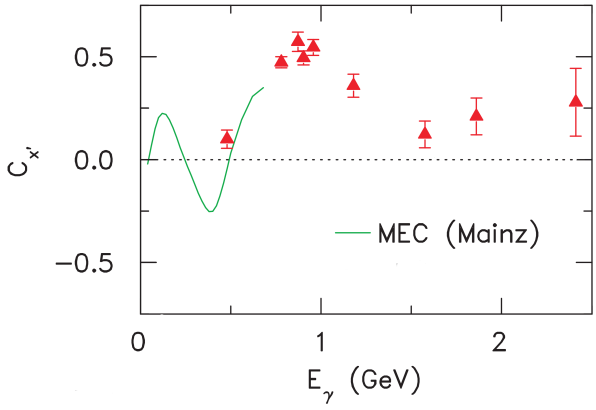

Figure 7: The polarisation transfer observable $C_{x'}^p$ as a function of incident photon energy for $\theta_p = 90°$. Data are from [41], the theoretical curve is from Schwamb and Arenhövel.

interest. Some data were taken on the inverse radiative capture reaction $\vec{n}p \rightarrow D\gamma$ at TRIUMF [45] the results of which can be seen in figure 6 compared to the calculations of Schwamb and Arenhövel [1]. The energy of the reaction is equivalent to an incident photon energy of 240 MeV. The data are reasonably well described by the calculations both qualitatively and quantitatively with a slight possible under-prediction of the asymmetry at larger θ_p though the statistical errors on the data there are poorer. At higher incident photon energies the calculations predict similar behaviour for the P_y^n and P_y^p asymmetries at $\theta = 90°$ see figure 5.

For polarisation transfer measurements some data have been taken to study $C_{x'}^p$ and $C_{z'}^p$ at JLab in two separate measurements to cover a range of angles and energies [41, 42]. Figure 7 shows data from the measurement of $C_{x'}^p$ at $\theta_p = 90°$ compared to the calculations of Schwamb and Arenhövel [1]. Most of the data points are for higher incident photon energies than where the calculations are applicable but where they are of low enough energy there is reasonable agreement between the calculations and data. At the limit of the calculated asymmetry, ∼700 MeV the theory predicts an increasing asymmetry which is seen in the data for the points around 1 GeV.

We propose to measure P_y^n and $C_{x'}^n$ over an incident photon energy range of 200 to 800 MeV at $\theta_n = 90°$. Such information will help the development of an improved theoretical description of the deuteron which will also help with analysis of data where it is used as a quasi-free neutron target. Links with various theoretical groups have been established for interpretation of the data. M. Schwamb has made improvements to his model that are as yet unpublished which extend his approach to include seven reactions simultaneously and are more rigorous with respect to the number of free parameters [46]. The Moscow-Tübingen theory group are also interested in using deuteron photo-disintegration as a testing ground for development of their model. The Jülich theory group are interested in developing and testing calculations based χPT.

2 Experimental issues

The proposed measurement would be carried out in the experimental area downstream of the Crystal Ball (CB) and would be completely independent of this and and the other detectors and electronics associated with it. The Glasgow tagger will be read out using spare logic outputs coupled to new multi-hit VMEbus TDCs purchased by Glasgow. On one side of the beam a set of analyser and polariser detectors measure the polarisation of the neutron whilst on the opposite side a proton detection system will be used to guarantee that only two-body reactions are observed. A sketch of the proposed set-up can be seen in figure 8. Both the ejected neutron and proton from the reaction would be detected in the measurement. The proton would be detected with good position and reasonable energy resolution to effectively 'tag' the ejected neutrons and compensate for the relatively poor neutron energy resolution due to the short flight distance to the analyser bars. Monte Carlo simulations of the proposed experimental set-up are currently being developed.

2.1 Kinematics

We wish to measure P_y^n and $C_{x'}^n$ at $\theta = 90°$ for a wide range of incident photon energies and to do this detector coverage of an in-plane angular range of $60° \leq \theta_{p/n} \leq 85°$ in the lab is necessary, see figure 9. The red curve in figure 9 is for $\theta = 90°$, the contours are from the expected incident photon flux assuming a $1/E_\gamma$ dependence on the flux in the tagger. As can be seen in the figure using such a set-up the two-body break-up at $\theta = 90°$ is completely covered in both frames for the whole incident photon energy range.

2.2 Detectors

2.2.1 Glasgow Photon Tagger

To tag the Bremsstrahlung photons the tagger in the A2 hall would be used [47, 48, 49]. For the measurement incident electron energies of 855 MeV are required. At such energies the main focal-plane detector of the tagger has a photon energy resolution of ~2MeV. A polarised electron beam will be required to produce circularly polarised photons to allow simultaneous measurement of both P_y^n and $C_{x'}^n$. For optimal conditions several energy settings are required. However when running in the parasitic mode coordination with the second experiment might dictate different energies at the benefit of longer measuring times.

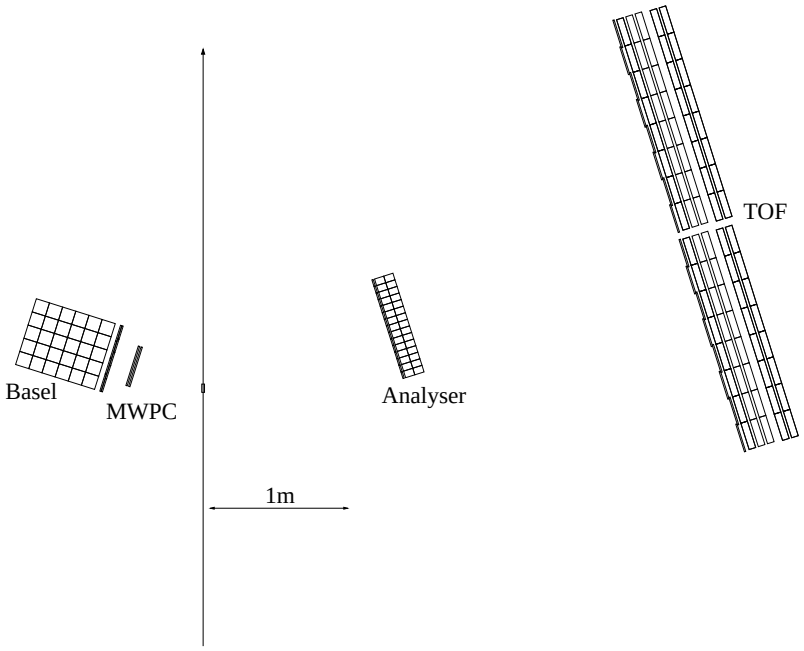

Figure 8: Plan view of the proposed experimental set-up. On the right-hand side a set of analyser detectors would be used to scatter the ejected neutrons which would then be detected again in some TOF bars. On the left MWPCs would be used to accurately determine the proton trajectory with scintillator detectors behind these for discrimination of protons and pions.

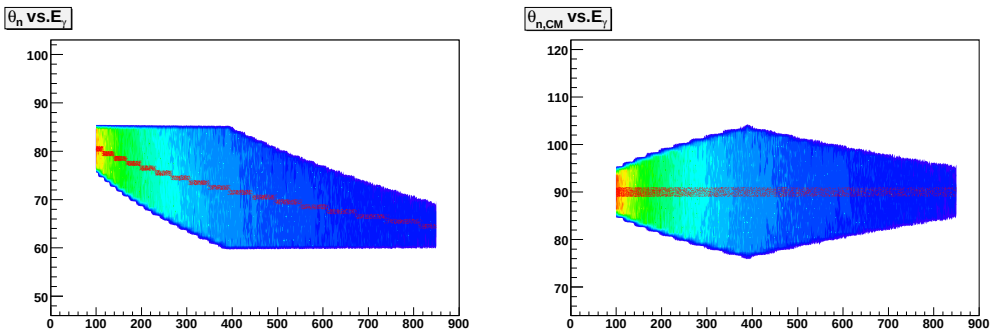

Figure 9: The $\theta_{n,Lab}$ and $\theta_{n,CM}$ dependence on E_γ for an in-plane angular acceptance of $60^\circ \leq \theta_{Lab} \leq 85^\circ$, the red curve is $\theta_{CM} = 90^\circ$.

2.2.2 Analyser Detectors

A set of scintillator detectors previously used for a measurement of G_e^n with the $^2\mathrm{H}(\vec{e}, e'\vec{n})$ reaction [50] will be used as the analyser for this measurement. The bars are $50 \times 75 \times 800$ mm in dimension and will be arranged on one side of the beam line in a frame of two layers as shown in figure 8. A layer of veto detectors would be placed in a frame in front of the two analysing layers to distinguish charged particles from neutral. The analyser detectors would be positioned at an angle of 72.5° in the lab at a distance of 1m from the target which would give an angular resolution of $\delta\theta = \delta\phi \approx 3°$ in both the horizontal and vertical directions.

2.2.3 TOF Detectors

The Glasgow-Tübingen TOF detector system [51] would be used to measure neutron scattering asymmetries. The TOF detector system consists of bars of plastic scintillator of $5 \times 20 \times 300$ cm^3 and $1 \times 22 \times 300$ cm^3 bars for charged particle identification. The bars are mounted vertically on frames in sets of eight and these frames are mounted on stands of up to four layers. Two stands of TOF detectors would be used side-by-side as the polariser with a front frame of veto detectors mounted in front of three frames of TOF bars. Directly behind these would be positioned further stands with more frames of TOF bars to improve the detection efficiency for the recoiling neutron. The front TOF stands would be positioned at a distance of roughly 3.5 m from the target giving an angular resolution of $\delta\theta \approx 3.3°$ and $\delta\phi \approx 1.7°$ in the horizontal and vertical directions respectively. The two TOF stands would be centred at 60° and 85° with respect to the incident photon direction.

2.2.4 Basel Detector

The Basel detector is a scintillator detector which consists of six layers of $10 \times 10 \times 50$ cm^3 scintillator bars mounted vertically in frames of five with a front frame of two overlapping veto layers, one of which consists of five $1 \times 10 \times 50$ cm^3 bars and the other of four $1 \times 12.5 \times 50$ cm^3 bars [52]. The frames are mounted in a purpose built stand. The thick bars have a position resolution of ≈ 3 cm in the vertical direction and with the detector positioned at a distance of 70 cm from the target this would give horizontal and vertical resolutions of $\delta\theta \approx 8°$ and $\delta\phi \approx 2.5°$ respectively. This detector will be used for triggering purposes on the proton side and for discrimination between protons and charged pions.

2.2.5 Multi-Wire Proportional Chambers

For determination of the trajectory of the proton and partial vertex reconstruction two layers of multi-wire proportional chambers (MWPC) [53] would be positioned in front of the Basel detector. Each MWPC consists of two perpendicular planes of 128 wires and has a sensitive area of 29.2×29.2 cm^2. They would be positioned at a distance of 50 cm from the target which would give an angular resolution of $< 1°$ in both the horizontal and vertical directions.

Accurate determination of the proton trajectory and knowledge of the incident photon energy will mean that the complete reaction kinematics of a given event can be reconstructed. This will allow the ejected neutrons four-vector to be determined and kinematic cuts be applied to the neutrons which should reduce the accidental background during the analysis of the data.

2.3 Target

The target would be a 10 cm long liquid deuterium target. A new target cell with a large surface area in the beam line will be produced to accommodate the size of the photon beam spot at the second target area. This will allow all of the collimated photons to pass through the target and give a tagging efficiency of $\sim$0.5.

2.4 Data Acquisition System

The experimental set-up will have its own data acquisition system independent of that currently in use for the CB-TAPS set-up including a separate set of tagger electronics. Enquiries have been made regarding this and all the modules necessary are available. This independent acquisition system will allow the proposed measurement to be made without affecting any of the current set-up in place for use with CB-TAPS. It also allows the possibility of running the measurement parasitically while other measurements are being made using the CB.

2.5 Analysing Power of Scintillator Detectors/Analyser

The beam time estimate below has been determined using the expected analysing power for elastic $\vec{n}-p$ scattering for the expected range of neutron kinetic energies and angular acceptance of the analyser and polariser detectors using data from the SAID data base [54]. In addition to elastic $\vec{n}-p$ scattering there will also be various quasi-elastic $\vec{n}+C$ reactions which make a contribution to the observed $(\vec{n},n')$ yield and thus change the effective analysing power of the scintillator, $\mathcal{A}_{\text{eff}}$. In a measurement of $\mathcal{A}_{\text{eff}}$ for plastic scintillator [55] it was found that the effective analysing power of the material was 70 % of that of the elastic $\vec{n}-p$ taken from the SAID data base. In the beam time estimate the analysing power taken from SAID has been reduced by a factor 0.7 to reflect this expected reduction in $\mathcal{A}_{\text{eff}}$.

Some time has been allocated to measure $\mathcal{A}_{\text{eff}}$ of the analyser detector during the beam time. For this measurement the detector roles will be reversed with the proton being detected in the analyser-polariser side of the set-up and the neutron in the Basel detector, the drift chambers shall be moved in front of the analyser detectors. Data will then be taken using the ejected protons to measure $\mathcal{A}_{\text{eff}}$ for the scintillator. The detection of the neutron in the Basel detector is not strictly necessary as the kinematics of a given reaction will be able to be completely reconstructed using the proton trajectory and tagged photon energy.

3 Event Rates and Beamtime Estimate

For the measurement we are aiming for a statistical precision of ≤ 0.1 in the absolute value of the measured asymmetry for P_y^n for 20 MeV bins in incident photon energy for the range $200 \leq E_\gamma \leq 800$ MeV. The statistical precision in C_x^n will be lower because of the degrees of electron and photon polarisation but is expected to range between 0.1 and 0.2 for the same bin size over the incident photon energy range. The assumptions used to determine the beam time necessary are as follows:

- Electron beam energy: $E_e = 855$ MeV.
- Electron beam polarisation of 80 %.

- Measurements at photon energy ranges: E_γ =200 - 500, 400 - 800 and 500 - 800 MeV.
- Tagging efficiency: $\epsilon_{tag} = 0.5$ for an incident electron energy of $E_e = 855$ MeV.
- Photon flux: $N_e = 0.25$ MHz/MeV at lowest photon energy with $1/E_\gamma$ dependence on flux of higher energy photon bins.
- Energy dependent circular polarisation of photon beam.
- Neutron detection efficiency: $\epsilon_n = 0.6$ %/cm in plastic scintillator.
- Proton detection efficiency: $\epsilon_p = 90$ %.
- Trigger condition: proton + neutron (analyser) + neutron (polariser).
- Analysing power: Energy dependent $\mathcal{A}_{\text{eff}}$ used based on elastic $\vec{n}-p$ scattering which is the mean of possible angular acceptance of set-up taking into account a reduction due to quasi-elastic$\vec{n}+C$ events
- Live time of 80 % in the electronics.

With the above numbers we estimate beamtime requirement of 450 hours including time for testing and determination of $\mathcal{A}_{\text{eff}}$ with a further 100 hours for the set-up. Details are given in table 1 below.

Setting	Time [hr]
$200 \leq E_\gamma \leq 500$	100
$400 \leq E_\gamma \leq 800$	100
$500 \leq E_\gamma \leq 800$	100
$\mathcal{A}_{\text{eff}}$	50
Empty Target	50
Tests	50
Set-up	100
Total	550

Table 1: Beam time request.

References

[1] M. Schwamb and H. Arenhövel. *Nucl. Phys. A*, 690:682, 2001.

[2] A. Deltuva et al. *Phys. Rev. C*, 70:034004, 2004.

[3] J. Golak, R. Skibiński, H. Witała, W. Glöckle, A. Nogga, H. Kamada. *Phys. Rept.*, 415:89, 2005.

[4] W. Glöckle, H. Witala, D. Hüber, H. Kamada and J. Golak. *Phys. Rep.*, 274:107, 1996.

[5] D. L. Groep et al. *Phys. Rev. C*, 63:014005, 2000.

[6] D.G. Middleton et al. Investigation of the Exclusive ^{3}He$(e,e'pn)p$ Reaction. arXiv:0903.1215, submitted to Phys. Rev. Lett.

[7] P. Achenbach et. al. *Eur. Phys. J. A*, 25:177, 2005.

[8] H. Arenhövel and M. Sanzone. *Photodisintegration of the deuteron.* Springer-Werlag, 1991.

[9] R. Gilman and Franz Gross. *J. Phys G*, 28:R37, 2002.

[10] M. Schwamb et al. *Phys. Lett. B*, 420:255, 1998.

[11] M. Schwamb and H. Arenhövel. *Nucl. Phys. A*, 696:556, 2001.

[12] Y. Kang, P Erbs, W. Pfeil and W. Rollnik. In *Abstracts of the Particle and Nuclear International Conference*. MIT Press, 1990.

[13] Y. Kang. PhD thesis, Bonn, 1993.

[14] V.I. Kukulin et al. *J. Phys. G*, 27:1851, 2001.

[15] V.I. Kukulin et al. *J. Phys. G*, 30:287, 2004.

[16] V.I. Kukulin et al. *J. Phys. G*, 30:309, 2004.

[17] V.I. Kukulin et al. *Phys. Rev. C*, 77:041001, 2008.

[18] V.I. Kukulin, I.T. Obukhovsky, P. Grabmayr, and A. Faessler. *Phys. Rev. C*, 74:064005, 2006.

[19] V.I. Kukulin, I.T. Obukhovsky, V.N. Pomerantsev, and A. Faessler. *Int. J. Mod. Phys. E*, 11:1, 2002.

[20] V.I. Kukulin and M.A. Shikhalev. *Phys. At. Nucl.*, 67:1558, 2004.

[21] Private communication.

[22] R. Crawford et al. *Nucl. Phys. A*, 603:303, 1996.

[23] J. Arends et al. *Nucl. Phys. A*, 412:509, 1984.

[24] G. Blanpied et al. *Phys. Rev. C*, 52:R455, 1995.

[25] G. Blanpied et al. *Phys. Rev. C*, 61:024604, 2000.

[26] S. Wartenberg et al. *Few-Body Systems*, 26:213, 1999.

[27] F. Adamian et al. *J Phys. G*, 17:1189, 1991.

[28] F.F. Liu et al. *Phys. Rev.*, 165:1478, 1968.

[29] R. Kose et al. *Z. Phys.*, 220:305, 1969.

[30] T. Kamae et al. *Nucl. Phys. B*, 139:394, 1978.

[31] H. Ikeda et al. *Phys. Rev. Lett.*, 42:1321, 1979.

[32] A.S. Bratashevskii et al. *Sov. J. Phys.*, 31:444, 1979.

[33] A.S. Bratashevskii et al. *Sov. J. Phys.*, 32:216, 1980.

[34] A.S. Bratashevskii et al. *JETP Lett.*, 34:389, 1982.

[35] A.S. Bratashevskii et al. *JETP Lett.*, 36:216, 1982.

[36] A.S. Bratashevskii et al. *Sov. J. Phys.*, 43:499, 1986.

[37] A.S. Bratashevskii et al. *Sov. J. Phys.*, 44:619, 1986.

[38] V.P. Barannik et al. *Nucl. Phys. A*, 451:751, 1986.

[39] A.A. Zybalov et al. *Nucl. Phys. A*, 533:642, 1991.

[40] V.B. Ganenko et al. *Z. Phys. A.*, 341:205, 1992.

[41] K. Wijesooriya et al. *Phys. Rev. Lett.*, 86:2975, 2001.

[42] X. Jiang et al. *Phys. Rev. Lett.*, 98:182302, 2007.

[43] H. Ikeda et al. *Nucl. Phys. B*, 172:509, 1980.

[44] M. Schwamb. Private communication.

[45] M. Hugi et al. *Nucl. Phys. A*, 472:701, 1987.

[46] M. Schwamb. Submitted to Phys. Rep.

[47] I. Anthony et al. *Nucl. Instr. and Meth. in Phys. Res. A*, 301:230, 1991.

[48] S.J. Hall et al. *Nucl. Instr. and Meth. in Phys. Res. A*, 368:698, 1996.

[49] J.C. McGeorge et al. *Eur. Phys. J. A*, 37:129, 2008.

[50] D.I. Glazier et al. *Eur. Phys. J. A*, 24:101, 2005.

[51] P. Grabmayr et al. *Nucl. Instr. and Meth. in Phys. Res. A*, 402:85, 1998.

[52] M. Distler, W. Heil, D.Rohe (spokespersons). A1-1/05 proposal at MAMI, 2005.

[53] J. Ahrens et al. *Eur. Phys. J. A*, 23:113, 2005.

[54] I.I. Strakovsky R.A. Arndt and R.L. Workman. *Phys. Rev. C*, 62:034005, 2000. http://gwdac.phys.gwu.edu/.

[55] T. Wakasa et al. *Nucl. Instr. and Meth. in Phys. Res. A*, 547:569, 2005.